

Inelastic Electron-Deuteron Scattering Experiments and Nucleon Structure*

C. DE VRIES,[†] R. HOFSTADTER, AND A. JOHANSSON[‡]

Stanford University, Stanford, California

AND

ROBERT HERMAN

Research Laboratories, General Motors Corporation, Warren, Michigan

(Received 23 December 1963)

Inelastic electron-scattering experiments are reported for four-momentum transfers from 3.0 to 22.0 F^{-2} . The results of these measurements have been combined with values of proton cross sections measured in the same region of q^2 and have been analyzed in terms of a three-pole Clementel-Villi model for the isotopic form factors. Parameters appearing in this model have been adjusted by statistical methods. The minimum values of χ^2 obtained show that the different blocks of information on elastic electron-proton and inelastic electron-deuteron cross sections measured at Stanford are consistent with each other. An important result of the analysis is that the cross sections cannot be fitted with only one $T=1$, $J=1$ multipion resonance, unless the effective mass of such a particle is taken to be approximately 600 MeV. This value is considerably lower than the accepted mass of the ρ resonance. On the whole the agreement with other data on the proton form factors and neutron form factors is rather good, although there is still some disagreement with results on the charge form factor of the neutron.

I. INTRODUCTION

IN the present paper we would like to give a more complete account of some earlier Stanford electron-deuteron scattering experiments which have been presented briefly during the last few years.¹⁻⁴ This experimental material and the experimental results on electron scattering on the proton⁵⁻⁸ have made it possible to give an interpretation of the nucleon form factors which appears to have a close connection with the theory of dispersion relations and strong pion-pion interactions.^{2,9,10}

Even though considerable progress has been made recently in the understanding of the electromagnetic structure of nucleons, there remain numerous unsolved problems in experiment and in theory. The solutions of these problems could turn out to be of great enough significance to change some details of our present views

of nucleon structure. To be specific, we wish to mention the following outstanding problems:

(a) Much of the present information on the neutron form factors has been obtained from studies of the inelastic scattering on the deuteron. The theory of the "peak method" (essentially a subtraction technique) of finding neutron form factors from the inelastic deuteron data has recently been improved. Nevertheless it has been derived under certain approximations which may or may not turn out to be valid. The influence of the final state interaction at the peak of the quasi-elastic deuteron curve is a matter of principal concern in this respect. It is possible also that there may be small meson-exchange contributions to this peak which have not been allowed for. Small modifications in the theory can seriously affect the numerical values of the neutron form factors.

(b) The Rosenbluth theory of the proton and neutron which has been the basis of the reduction of the elastic cross sections into form factors was derived on the assumption that only one virtual photon is exchanged during the scattering process. From recent results it is unlikely that this assumption will be invalidated, at least for the values of momentum transfer under present consideration. Nevertheless a rigorous proof of the assumption remains to be given. Theoretical considerations of this problem have been made by Drell and Ruderman¹¹ and by Drell and Fubini.¹²

(c) The experimental material on electron-proton cross sections of the Cornell^{13,14} and Stanford^{7,8} groups show slight systematic differences. As a result both the proton and neutron form factors contain uncertainties

* This work was supported in part by the U. S. Navy, Office of Naval Research, the U. S. Atomic Energy Commission, and the U. S. Air Force, Office of Scientific Research.

[†] Present address: Institute for Nuclear Research, Amsterdam, The Netherlands.

[‡] On leave from Gustaf Werner Institute, Uppsala, Sweden.

¹ R. Hofstadter, C. de Vries, and R. Herman, *Phys. Rev. Letters* **6**, 290 (1961).

² R. Hofstadter and R. Herman, *Phys. Rev. Letters* **6**, 293 (1961).

³ C. de Vries, R. Hofstadter, and R. Herman, *Proceedings of the Aix-en-Provence International Conference on Elementary Particles 1962* (Centre d'Etudes Nucléaires de Saclay, Seine et Oise, France, 1962), Vol. 1, p. 121.

⁴ C. de Vries, R. Hofstadter, and R. Herman, *Phys. Rev. Letters* **8**, 381 (1962).

⁵ F. Bumiller, M. Croissiaux, and R. Hofstadter, *Phys. Rev. Letters* **5**, 261 (1960).

⁶ R. Hofstadter, F. Bumiller, and M. Croissiaux, *Phys. Rev. Letters* **5**, 263 (1960).

⁷ F. Bumiller, M. Croissiaux, E. Dally, and R. Hofstadter, *Phys. Rev.* **124**, 1623 (1961).

⁸ T. Janssens, R. Hofstadter, E. B. Hughes, and M. R. Yearian (to be published).

⁹ S. Bergia, A. Stanghellini, S. Fubini, and C. Villi, *Phys. Rev. Letters* **6**, 367 (1961).

¹⁰ S. Bergia and A. Stanghellini, *Nuovo Cimento* **21**, 155 (1961).

¹¹ S. Drell and M. Ruderman, *Phys. Rev.* **106**, 561 (1957).

¹² S. Drell and S. Fubini, *Phys. Rev.* **113**, 741 (1959).

¹³ D. M. Olson, H. F. Schopper, and R. R. Wilson, *Phys. Rev. Letters* **6**, 286 (1961).

¹⁴ R. M. Littauer, H. F. Schopper, and R. R. Wilson, *Phys. Rev. Letters* **7**, 141 (1961).

due to these discrepancies. Thus further knowledge about the exact nature of the systematic sources of error might lead to a quantitative change in the numerical values of the form factors.

(d) A generalized Clementel-Villi^{2,9,10,15} model for the nucleon form factors has been used in the present analysis to give a theoretical interpretation of the experimental cross sections. This model could conceivably turn out to be inadequate as more precise numerical values of the form factors become available. The possible existence of other multipion vector resonances may also force one to modify this model.

It is clear that future developments could change the qualitative features of the picture of nucleon structure that we shall give in this paper. However, we feel that the general ideas outlined by Bergia *et al.*⁹ and by Hofstadter and Herman² on the electromagnetic structure of nucleons are substantially correct and we present the following material in this spirit.

II. MEASUREMENTS

Various methods are now available for obtaining information about the structure of the neutron. Among these are: elastic electron scattering from the deuteron, electroproduction of pions, and inelastic electron scattering from the deuteron. In this paper we have used the latter method, proposed by Hofstadter.¹⁶ It is based on the idea that because of the loose binding of the nucleons in the deuteron, the inelastic electron-deuteron cross section may be written mainly as a sum of the elastic electron cross sections of the proton and the neutron. It has been pointed out elsewhere¹⁷ that there are two different ways of employing the analyses of the electron-deuteron inelastic spectrum: The first method, called the "area method," determines the total cross section for a fixed value of the scattering angle and is therefore the integral of the double differential cross section $d^2\sigma/d\Omega dE$ extended over all energies (E) of the scattered electron. The second method, called the "peak method" determines the double differential cross section at the peak of the inelastic continuum of the deuteron. The theoretical situation is simplified considerably in this case because the scattered electrons behave as if they had been scattered approximately elastically from nucleons at rest. Detailed knowledge of the deuteron wave function is made less necessary because the average momentum of a nucleon is small and the nucleons are on the average far apart. Drell¹⁸ has also proposed that the meson-exchange contributions to the cross section might be small in the use of the peak method. The peak method has been used previously and we have continued to use it for the measurements reported in this paper. This means that although we measured the complete

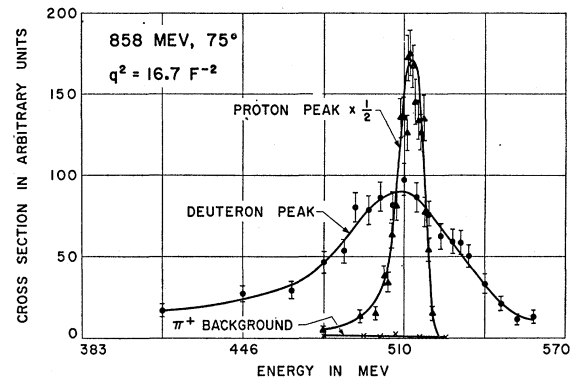


FIG. 1. Typical elastic electron-proton and inelastic electron-deuteron spectra as measured with the 72-in. magnetic spectrometer. Corrections for counting rates and differences in density between liquid hydrogen and deuterium are already applied to the experimental points. The spectra shown in this figure and in Fig. 2 are taken for the same value of the four-momentum transfer but for different values of primary energy and scattering angle.

inelastic spectrum in 38 of the 71 cases, only the points close to the peak were used to determine the value of the cross section at the peak. Consequently, no theory for the spectrum shape had to be used. For a discussion of the advantages and limitations of this method we refer the reader to Ref. 17.

The arrangement of the experiment has already been described in detail^{7,19} and we will restrict our remarks only to matters not presented previously.

The primary electron beam is obtained from the Stanford 1-BeV electron linear accelerator. The beam switching system at the end of the accelerator determines the energy and energy width of the beam entering the experimental area. After passing through the target, the beam is monitored by a Faraday cup. The position at which the beam passes through the target is controlled continuously by an operator who observes the image of the beam on a television screen. The scattered electrons are analyzed in momentum by means of the 72-in. magnetic spectrometer and are detected with a single liquid Čerenkov counter. Various properties and numerical characteristics of this apparatus, such as momentum calibration and dispersion of the magnetic field of the analyzing magnet, and efficiencies of the Faraday cup and Čerenkov counter, are discussed in Ref. 7.

It should be pointed out that several sources of systematic error do not enter into the measurements described in this paper because the information at the peak of the inelastic electron-deuteron spectrum is obtained relative to the elastic scattering data from the proton. Another reason for taking relative data, rather than absolute data, is that the target construction is not suitable for absolute measurements. This target,

¹⁵ E. Clementel and C. Villi, *Nuovo Cimento* 4, 1207 (1956).

¹⁶ R. Hofstadter, *Rev. Mod. Phys.* 28, 214 (1956).

¹⁷ R. Hofstadter, F. Bumiller, and M. R. Yearian, *Rev. Mod. Phys.* 30, 482 (1958).

¹⁸ S. D. Drell (unpublished).

¹⁹ R. Hofstadter, F. Bumiller, B. R. Chambers, and M. Croisiaux, *Proceedings of an International Conference on Instruments for High-Energy Physics* (Interscience Publishers, Inc., New York, 1961), pp. 310-315.

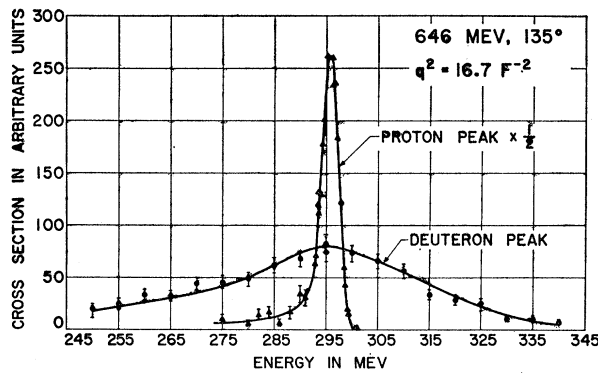


FIG. 2. The data in this figure are similar to those in Fig. 1.

which is similar to one used earlier,²⁰ consists of a cylindrical tube, $7\frac{1}{2}$ in. long, with a diameter of 1.0 in. The walls are 1-mil-thick stainless steel. The incident beam of electrons has a diameter of about $\frac{1}{4}$ in. and passes along the axis of the cylinder. This configuration makes certain that the scattering of the primary beam from the target walls is not viewed by the spectrometer and empty target background is avoided. On the other hand, it is very difficult to establish the actual target thickness viewed by the spectrometer. Therefore, we have used a dual target construction built up of two identical cylindrical tubes, one filled with liquid deuterium and the other filled with liquid hydrogen. These targets are brought alternatively into the primary beam line and two different measurements are taken during the same

run, providing data at the elastic scattering peak of the proton, and at the inelastic scattering peak of the deuteron.

The two examples of the original data in Figs. 1 and 2 show the elastic proton peak along with the main part of the inelastic continuum of the deuteron. The data were taken at two values of the primary energy and at different scattering angles but at the same value of the four-momentum transfer, $q^2 = 16.7 \text{ F}^{-2}$. There is essentially no background under the proton peaks. There is a background problem in the case of the deuteron because of the production of negatively charged pions. As in previous investigations, we have corrected for this background by measuring the number of positive pions and by determining the number of negative pions under the deuteron continua from the π^-/π^+ ratios measured by Neugebauer *et al.*²¹ We have to assume that electrons produce pions in the same ratio as photons of the appropriate energy. Since a fraction of the pions in our backgrounds are, indeed, produced by photons because of our use of a thick target, and since the backgrounds are usually only a small correction to the data we feel this procedure is justified. Recent Stanford data also support the assumption of equal π^-/π^+ ratios for electroproduction and photoproduction.

In a few cases where the pion background was not small this procedure led to larger possible errors, and we have used an additional technique to obtain the data. This is the technique of discrimination between the pulse heights of electrons and the smaller pulse heights of pions of the same momentum but different en-

TABLE I. Cross sections for electron scattering.

q^2 (F^{-2})	E (MeV)	$(d\sigma/d\Omega)_{\text{proton}}$ Rad. corr. coefficient	Total area (MeV counts)	$(d^2\sigma/d\Omega dE)_{\text{deuteron, peak}}$ Rad. corr. coefficient	Corrected height ^a (counts)	Ratio $(d\sigma/d\Omega)_p / (d^2\sigma/d\Omega dE)_d$ (MeV)
60°						
1.993	300	1.325	1190	1.165	44.5	26.8±1.9
2.652	350	1.325	1725	1.170	63.8	27.1±1.9
2.652	350 ^b					26.5
3.791	425	1.320	2180	1.170	63.8	34.2±2.1
4.633	475	1.322	2635	1.170	76.0	34.7±2.1
5.070	500 ^b					31.0
5.530	525 ^b	1.320	2110	1.160	67.4	31.3±2.2
6.008	550	1.275	7920	1.172	242.0	32.7±2.3
7.006	600 ^b					33.5
8.608	675	1.263	2920	1.155	79.6	36.7±2.2
9.166	700	1.250	2690	1.168	67.1	40.1±2.8
9.513	715	1.250	6660	1.172	179.5	37.2±1.9
9.744	725	1.250	4440	1.170	103.2	43.0±3.0
10.563	760	1.252	4840	1.175	119.0	40.6±2.0
11.525	800	1.252	7400	1.180	187.0	39.6±2.0
11.90	815	1.248	8800	1.182	211.5	41.6±2.1
12.77	850	1.245	7560	1.180	176.5	42.8±2.1
13.16	865	1.250	5000	1.180	120.5	41.5±2.1
13.42	875	1.250	11 000	1.182	274.5	40.1±2.4
14.06	900	1.245	10 160	1.165	230.5	44.1±3.1
14.72	925	1.248	2920	1.175	66.2	44.1±3.5
15.39	950	1.248	7850	1.170	188.0	41.8±2.9

²⁰ M. R. Yearian and R. Hofstadter, Phys. Rev. **110**, 552 (1958).²¹ G. Neugebauer, W. Wales, and R. L. Walker, Phys. Rev. **119**, 1726 (1960).

INELASTIC ELECTRON-DEUTERON SCATTERING EXPERIMENTS B851

TABLE I. (Continued).

q^2 (F^{-2})	E (MeV)	$(d\sigma/d\Omega)_{\text{proton}}$ Rad. corr. coefficient	Total area (MeV counts)	$(d^2\sigma/d\Omega dE)_{\text{deuteron, peak}}$ Rad. corr. coefficient	Corrected height ^a (counts)	Ratio $(d\sigma/d\Omega)_p / (d^2\sigma/d\Omega dE)_d$ (MeV)
75°						
3.21	325	1.290	1650	1.178	64.5	25.6±2.0
4.63	400	1.280	1040	1.175	35.9	29.9±2.4
5.69	450	1.272	4260	1.175	158.5	26.9±1.9
6.82	500	1.269	5400	1.160	166.0	32.6±1.6
8.03	550	1.269	5280	1.175	156.0	33.8±1.7
9.30	600	1.255	5148	1.170	151.0	34.0±2.0
9.30	600 ^b					35.0
10.63	650	1.262	5420	1.160	152.5	35.6±1.8
12.01	700	1.261	5180	1.175	144.5	35.9±2.2
13.45	750	1.262	5180	1.165	135.0	38.4±1.9
14.93	800	1.260	5560	1.155	146.5	38.0±2.6
18.02	900	1.248	4800	1.155	108.0	40.7±3.2
90°						
2.54	250	1.290	616	1.175	25.4	24.3±1.7
4.04	325	1.285	1345	1.165	47.0	28.8±2.3
5.76	400	1.280	1610	1.160	59.0	27.3±2.2
7.03	450	1.270	2690	1.162	91.5	29.4±2.
8.38	500	1.270	2990	1.154	103.0	29.1±2.1
11.28	600 ^b					31.2
12.82	650	1.270	2250	1.151	69.0	32.7±2.5
12.82	650 ^b					32.4
17.75	800	1.250	2730	1.132	73.0	37.4±2.5
21.24	900	1.275	880	1.120	22.0	39.7±4.0
21.24	900	1.262	3130	1.129	84.5	37.1±2.2
120°						
2.335	200	1.280	705	1.120	33.7	20.9±1.3
3.441	250	1.285	1360	1.115	58.8	23.2±1.4
4.687	300	1.280	1140	1.117	45.3	25.2±1.5
4.687	300	1.280	1185	1.117	48.6	24.4±1.7
5.369	325	1.285	1125	1.120	44.3	25.4±1.3
6.052	350	1.284	1190	1.120	46.0	25.8±1.3
6.786	375	1.282	740	1.125	27.4	26.9±2.1
7.520	400	1.285	1380	1.126	45.1	30.6±1.8
9.075	450	1.285	1495	1.125	57.0	26.3±1.6
10.706	500	1.280	1450	1.128	49.1	29.5±1.8
14.158	600	1.274	950	1.120	33.9	28.0±1.7
17.817	700	1.290	1470	1.127	50.1	29.3±1.8
21.639	800	1.280	1050	1.115	29.6	35.4±2.8
25.591	900	1.269	670	1.110	20.6	32.5±2.6
135°						
2.572	200	1.290	792	1.125	36.4	21.8±1.3
3.767	250	1.290	878	1.125	41.7	21.1±1.5
5.105	300 ^b					21.7
5.688	320	1.285	795	1.120	36.2	21.9±1.3
6.009	331	1.288	640	1.118	27.4	23.4±2.9
6.563	350 ^b					23.3
7.342	375	1.282	1135	1.122	48.8	23.2±1.2
8.942	425 ^b					25.1
9.764	450	1.288	1500	1.132	58.6	25.6±1.5
9.764	450 ^b					26.4
11.136	490	1.275	1930	1.110	72.9	26.5±1.6
11.48	500 ^b					29.1
11.73	507	1.272	1700	1.112	59.3	28.7±1.7
11.90	512	1.275	1640	1.102	56.5	29.0±1.7
12.19	520	1.275	1660	1.108	61.2	27.1±1.9
12.76	536	1.276	1740	1.108	64.2	27.1±1.9
13.26	550 ^b					27.9
13.42	554	1.275	1575	1.115	57.5	27.4±1.6
14.17	575	1.285	1450	1.120	51.5	28.2±2.0
14.72	590	1.320	940	1.109	33.0	28.7±2.3
15.09	600 ^b					28.0
15.39	608	1.295	650	1.119	23.5	27.7±2.2
16.86	647	1.288	1370	1.135	45.6	30.0±2.4
18.02	677	1.320	479	1.130	159.0	30.1±3.0

^a Height normalized to number of microcoulombs taken for the proton peak. Usually about 200 counts were taken at the peak of the inelastic deuteron peak spectrum.

^b Sobottka, Ref. 22.

ergy. By discriminating against pions at the expense of also losing some of the electrons we can measure relative numbers of electrons scattered from protons and deuterons. The bias is set high enough to eliminate positive pions and thus when the spectrometer polarity is reversed, the negative pions should be eliminated. We assume that the pulse-height spectra of electrons scattered from the proton target are identical with those scattered from the deuteron target. Hence it can be argued that the ratio

$$R = \left(\frac{d\sigma}{d\Omega} \right)_p / \left(\frac{d^2\sigma}{d\Omega dE} \right)_{d,\text{peak}}$$

which is of primary interest for the present paper will not be influenced. To test this method, we have made experimental checks at a few points and have shown that this ratio is independent of the discriminator setting.

The spectra in Figs. 1 and 2 are corrected for small counting rate losses and for the difference in densities of liquid hydrogen and liquid deuterium. Seventy-one different measurements of this kind have been made. The results of these measurements are given in Table I. We show the experimental ratio values, R , measured at five different scattering angles: 60, 75, 90, 120, and 135° at different values of q^2 covering the region of four-momentum transfer from 3.0 up to 22.0 F⁻². The limits of error lie between 5 and 8% and arise mainly from counting statistics. Systematic errors of the type discussed by Bumiller *et al.*⁷ cancel out in our relative measurements. The values in the table are also corrected for radiative effects. The expressions used for the radiative corrections are those calculated by Sobottka.²² Tsai²³ has calculated improved values of the radiative corrections in the case of electron-proton collisions. Similar calculations have been made very recently by Meister and Griffy²⁴ for the process of inelastic electron-deuteron scattering. The radiative corrections to our ratio values resulting from the calculations of Tsai and of Meister and Griffy are not significantly different from those we have applied.

For comparison we have also quoted ratios in Table I which are derived from the work by Sobottka.²² The agreement is satisfactory. In the present paper we have not allowed for corrections to the height of the inelastic deuteron peak due to the interactions between the outgoing nucleons. We will discuss the final-state interactions in the next section.

III. FINAL-STATE INTERACTION

Durand²⁵ has shown that a number of relativistic corrections can be calculated rather easily at the peak of the inelastic continuum. However, the peak method introduces a complication first considered by Jankus.²⁶ This complication in the theory involves the interaction in the final state between the outgoing nucleons. Jankus estimated the influence of the final-state interaction on the inelastic spectrum of the deuteron and used a central force model for the p - n interaction. His results at two different values of q^2 (1.08 F⁻² at 70° and 2.65 F⁻² at 60°) indicate that the changes in $(d^2\sigma/d\Omega dE)_{d,\text{peak}}$ where quite small in the region of the quasi-elastic peak. This was due mainly to the cancellation of the contributions of the different waves (S , P , D , F , etc.) considered in his analysis. Durand has verified that the total correction to the peak cross section is small, partly due to the cancellation of the effects of the S , P , and D waves. He obtained these results by using for each particular case an "equivalent square well" potential which generates the experimental p - n phase shifts. His calculations were made for $q^2=6.76$ F⁻² and for $q^2=11.56$ F⁻² for scattering angles varying from 45 to 135°.

Durand suggests that a uniform correction of minus 2% should be applied to the theoretical values of the cross section at the peak of the inelastic continuum of the deuteron. We have found that the numerical values of the neutron form factors are quite insensitive to the suggested correction because it is a constant percentage of the peak cross section for the different scattering angles at which the experiments are performed and thus its effect tends to cancel out.

A different type of approach to this problem was made by Bosco.²⁷ This author applied the method of dispersion relations and evaluated appropriate matrix elements using experimental phase shifts in his analysis. Free parameters appearing in the formulas for the S -wave matrix elements were determined from the experiment of Kendall *et al.*²⁸ on the inelastic cross section near threshold where the effect of the S wave predominates. Bosco²⁹ calculates the corrections corresponding to the final-state interaction of the S -wave contribution to the quasielastic peak. The correction is added to the Born approximation contribution of the S -wave final-state interaction. Applying these corrections and neglecting corrections due to waves with $l>0$ can have a considerable effect on the neutron form factors.³

Recently Nuttall and Whippman³⁰ have made more accurate calculations basically along the same lines as Durand; the Gammel-Thaler potential is used to describe the neutron-proton interaction. They find the

²² S. Sobottka, Phys. Rev. **118**, 831 (1960); Ph.D. thesis, Stanford University, 1960 (unpublished).

²³ Y. S. Tsai, Phys. Rev. **122**, 1898 (1961); straggling corrections are not included in Tsai's paper.

²⁴ N. Meister and T. Griffy, in *Proceedings of the Conference on Nuclear Structure* (Stanford University Press, Stanford, California, 1963).

²⁵ L. Durand, III, Phys. Rev. Letters **6**, 631 (1961); Phys. Rev. **123**, 1393 (1961).

²⁶ V. Z. Jankus, Phys. Rev. **102**, 1586 (1956).

²⁷ B. Bosco, Phys. Rev. **123**, 1072 (1961).

²⁸ H. W. Kendall, J. I. Friedman, E. F. Erickson, and P. A. M. Gram, Phys. Rev. **124**, 1596 (1961).

²⁹ B. Bosco and R. B. De Bar, Nuovo Cimento **26**, 604 (1962).

³⁰ J. Nuttall and M. L. Whippman, Phys. Rev. **130**, 2495 (1963).

corrections to be somewhere in between those of Durand and Bosco.

Since there is some disagreement between the various calculations we prefer to present our data without applying any correction for the final-state interaction. Also, there is one important conclusion to be drawn from all the theoretical work that has been carried out so far: the rescattering corrections are small for $q^2 \geq 8.0 \text{ F}^{-2}$. Thus for most of the numerical values of the neutron form factors in the region of q^2 under consideration, the effect of these corrections can be neglected with confidence. As more experiments are made in the future the effects of the final-state interactions will have to be included.

IV. ANALYSIS OF THE EXPERIMENTAL MATERIAL

The theoretical expression for the cross section at the peak of the inelastic electron-deuteron spectrum is given by Durand²⁵:

$$\left(\frac{d^2\sigma}{d\Omega dE}\right)_{d,\text{peak}} = \sigma_{\text{Mott}}(4.6 \times 10^{-3}) \times [t(1+t)]^{-1/2} [G_p + G_n], \quad (1)$$

where $t = q^2/4M^2$, and G_p and G_n are the expressions for electron scattering from a free proton and a free neutron, respectively, given by Rosenbluth³¹:

$$G_{\text{nucleon}} = (d\sigma/d\Omega)_{\text{nucleon}}/\sigma_{NS} = (1+t)^{-1} \times [G_e^2 + \{t + 2t(1+t) \tan^2(\frac{1}{2}\theta)\} G_m^2]. \quad (2)$$

Formula (1) does not contain the influence of final-state interactions and therefore differs slightly from the expression given by Durand.

G_p and G_n are functions of the invariants $G_e(q^2)$ and $G_m(q^2)$, the charge and magnetic form factors of the nucleons. An alternative presentation of G_p and G_n can be given in terms of the Dirac- (F_1) and Pauli- (F_2) form factors. Originally, the set F_1, F_2 was uniformly used, but recently the form factors G_e, G_m , which are linear combinations of F_1 and F_2 , have received much attention by different authors.^{32,33} We do not know if the dispersion relations should be applied to G_e and G_m or to F_1 and F_2 , but for convenience of comparison with recent authors we have adopted the electric and magnetic form factors to present the results of the experiment under consideration.

It is well known that the separate numerical values of the form factors can be obtained by plotting at constant q^2 the experimental quantities G_p (or G_n) as a function of $\tan^2 \frac{1}{2}\theta$. In such a plot the slope and intercept of the straight line fitted to the data determine the form factors [see Eq. (2)]. In earlier publications we proceeded to analyze the form-factor spectra thus obtained in terms of theoretical models. In the present paper we

start with a theoretical model of the form factors and compute the cross sections, which are compared point by point with the experimental material. The free parameters appearing in the model are adjusted so that a minimum of χ^2 is obtained. This technique is more direct, treats all experimental data uniformly and avoids smoothing procedures which often had to be used in earlier analyses in order to obtain the form-factor spectra. On the other hand, the results will be biased by the particular model used. Because the theoretical foundation for the model is rather well established, and because the number of parameters is quite large we believe, however, that this bias is small.

The following theoretical model for the isotopic form factors has been used:

$$\begin{aligned} G_e^S &= 0.50 \left\{ \frac{s_{e1}}{1+q^2/15.6} + \frac{s_{e2}}{1+q^2/26.6} + (1-s_{e1}-s_{e2}) \right\}, \\ G_e^V &= 0.50 \left\{ \frac{v_{e1}}{1+q^2/M_\rho^2} + (1-v_{e1}) \right\}, \\ G_m^S &= 0.44 \left\{ \frac{s_{m1}}{1+q^2/15.6} + \frac{s_{m2}}{1+q^2/26.6} + (1-s_{m1}-s_{m2}) \right\}, \\ G_m^V &= 2.353 \left\{ \frac{v_{m1}}{1+q^2/M_\rho^2} + (1-v_{m1}) \right\}. \end{aligned} \quad (3)$$

The proton and neutron form factors are obtained from the isotopic form factors as follows:

$$\begin{aligned} G_{ep} &= G_e^S + G_e^V, \\ G_{mp} &= G_m^S + G_m^V, \\ G_{en} &= G_e^S - G_e^V, \\ G_{mn} &= G_m^S - G_m^V. \end{aligned} \quad (4)$$

The isotopic form-factor model is based on the ideas of dispersion theory and of strong pion-pion interactions (two-pion and three-pion resonances). The resonances used here are the ($T=0, J=1$) three-pion states ω (15.6 F^{-2}) and ϕ (26.6 F^{-2}), and the ($T=1, J=1$) two-pion state, $\rho(M_\rho^2)$. The first two resonances manifest themselves in the isoscalar form factors, G_e^S and G_m^S , whereas the third resonance contributes to the isovector form factors, G_e^V and G_m^V .

The formulas in Eq. (3) are approximate in the sense that the resonances are considered to be delta functions in the integrand of the more accurate form factor expression:

$$G_{e,m}^{S,V} = \frac{1}{\pi} \int_a^\infty \frac{g(t') dt'}{t'-t}, \quad (5)$$

where $t = q^2$ and where the lower limit a depends on the mass of the pion.⁹

³¹ M. N. Rosenbluth, Phys. Rev. **79**, 615 (1950).

³² F. J. Ernst, R. G. Sachs, and K. C. Wali, Phys. Rev. **119**, 1105 (1960).

³³ L. N. Hand, Phys. Rev. **129**, 1834 (1963).

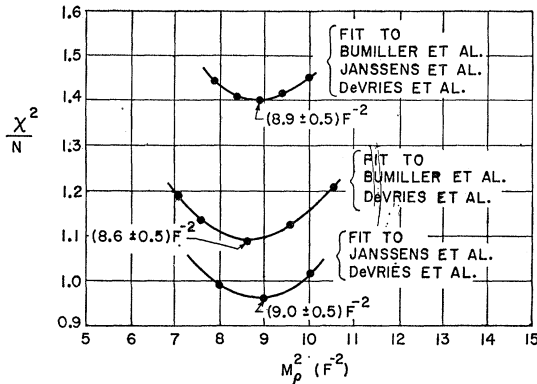


FIG. 3. The figure shows the behavior of χ^2 as a function of one of the six free parameters used in the statistical analyses, namely M_ρ^2 . Three curves are shown which correspond to the results of the statistical analyses on the combinations of data sets a, b, and c (see text).

The actual values of χ^2 are normalized by dividing by the number of degrees of freedom, N . Each point indicated corresponds to a completely independent analysis, in which a minimum is sought by varying the numerical values of the remaining five free parameters in the theoretical model [Eq. (3)].

This approximation is very good for the scalar resonances ω and ϕ (780 ± 10) MeV and (1019 ± 2) MeV, respectively, but the ρ resonance appears as a broad peak, (750 ± 100) MeV. As has been pointed out by Kirson,³⁴ this peak can be replaced to a good approximation by a sharp resonance at a somewhat lower energy than 750 MeV. Scotti and Wong³⁵ in their analysis of the nucleon-nucleon interaction that the effective position of the ρ mass is about 600 MeV. These two considerations have led us to take the mass of the ρ resonance as a free parameter in our analysis. Hence, we have seven free parameters in the model but we reduce the number to six by using the neutron-electron result³⁶:

$$\left(\frac{dG_{en}}{dq^2} \right)_{q^2=0} = 0.021 F^2. \quad (6)$$

The constant terms in Eq. (3) stand either for hard cores in the structure of the nucleons or for higher mass states whose q^2 dependence is not noticeable in the region of four-momentum transfer under consideration. We have refrained from inserting any further assumptions in the model. For instance, no resonances have been employed other than those known at present. Also we have not used constraints such as those proposed by Sachs³⁷ concerning the high-energy behavior of the form factors.

From Eq. (1) it is evident that proton cross sections are needed to derive neutron cross sections from the inelastic electron-deuteron scattering experiments. In

³⁴ M. W. Kirson, Phys. Rev. **132**, 1249 (1963).

³⁵ A. Scotti and D. Y. Wong, in *Proceedings of the Conference on Nucleon Structure* (Stanford University Press, Stanford, California, 1963).

³⁶ D. J. Hughes, L. A. Harvey, M. D. Goldberg, and M. J. Stafne, Phys. Rev. **90**, 497 (1953).

³⁷ R. G. Sachs, Phys. Rev. **126**, 2256 (1962).

the q^2 region of interest two sets of proton cross section exist which have been used in the present analyses: data set I: 58 points as measured by Bumiller *et al.*⁷; and data set II: 114 points as measured by Janssens *et al.*⁸ The latter set is the most recent one and has been obtained with improved techniques and new liquid hydrogen targets instead of CH_2 targets. A comparison of the two sets of data shows rather good agreement. The only significant difference appears at large angles where the cross sections obtained by Janssens *et al.*, are systematically somewhat higher than those measured by Bumiller *et al.* As we have no way of preferring one set over the other we have processed both sets in the analysis. There are several additional data sets known for the proton cross sections which could have been included. However, those used here represent most of the total material available for $q^2 \leq 32 F^{-2}$ and it is our opinion that the conclusions of this paper will not require substantial changes if a more complete analysis were made. Results of such an analysis, including most known electron-nucleon cross sections, will be reported in a forthcoming paper.

We shall label the set of 71 deuteron data points of the present paper as data set III. The results quoted below refer to the following combinations of data sets:

Combination a: data set I combined with data set III;
Combination b: data set II combined with data set III;
Combination c: data sets I, II, and III.

The IBM-7090 computer at Stanford University was used to adjust the free parameters in the expressions for the isotopic form factors of Eq. (3) in order to obtain a best fit. The search logic to find the minimum χ^2 was

TABLE II. Fits of the three-pole isotopic form factor model.

	Combination a: Bumiller <i>et al.</i> (58 points) de Vries <i>et al.</i> (71 points)	Combination b: Janssens <i>et al.</i> (114 points) de Vries <i>et al.</i> (71 points)	Combination c: Bumiller <i>et al.</i> (58 points) Janssens <i>et al.</i> (114 points) de Vries <i>et al.</i> (71 points)
s_{e1}	4.21	2.89	3.12
s_{e2}	-4.32	-2.30	-2.63
s_{m1}	5.86	5.13	4.65
s_{m2}	-5.68	-4.72	-4.07
v_{e1}	1.29	1.26	1.27
v_{m1}	1.11	1.09	1.09
M_ρ^2	8.6 F^{-2}	9.0 F^{-2}	8.9 F^{-2}
χ^2 Bumiller	84.5	(180.6) ^a	145.0
χ^2 Janssens	(707.8) ^a	120.8	134.4
χ^2 de Vries	50.0	50.8	52.9
χ^2 Total	134.5	171.6	332.3
$N = \text{No. of}$	123	179	237
degrees of			
freedom			
χ^2/N	1.09	0.96	1.40

^a Note that these entries are not included in χ^2 total, i.e., they have not been used in the minimizing of χ^2 .

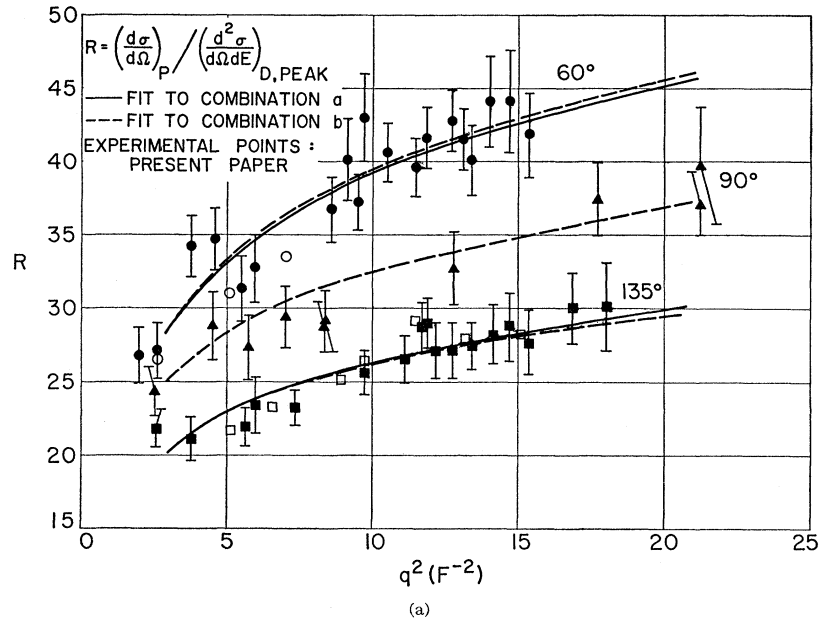
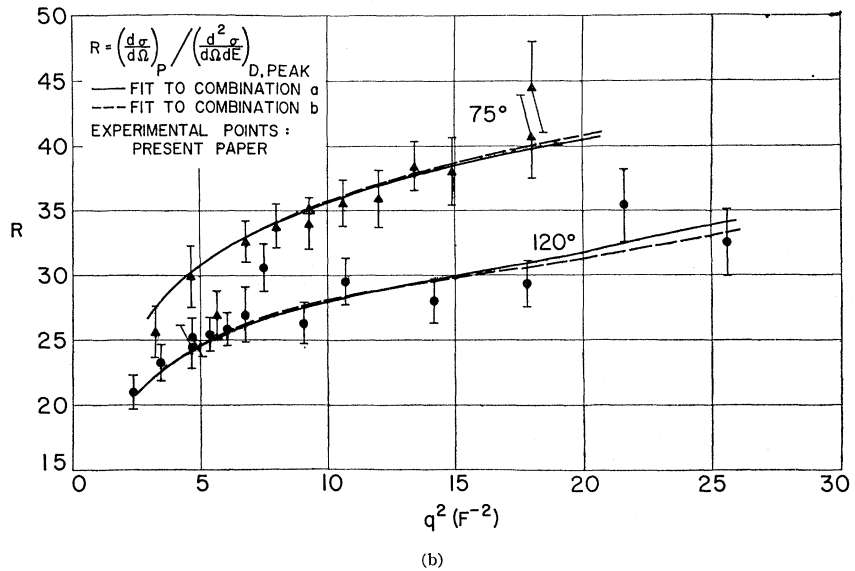


FIG. 4. (a) The experimental quantity

$$R = \left(\frac{d\sigma}{d\Omega} \right)_p / \left(\frac{d^2\sigma}{d\Omega dE} \right)_{d, \text{peak}}$$

is plotted as a function of the four momentum transfer, q^2 . The points shown (full symbols) correspond to the values of R in Table I for the scattering angles 60, 90, and 135°. The values indicated by the open symbols are derived from the work of Sobottka (Ref. 22). The curves for combination a and combination b refer to the data obtained from the statistical analyses described in the text. (b) This figure is similar to Fig. 4(a) and contains the results for 75 and 120°.



kindly supplied to the authors by P. Noyes and has been further developed in this work. We did not explore the complicated dependence of χ^2 on the free parameters well enough to claim that the values we find are unique; other values for the parameters may give acceptable values of χ^2 . However, we believe that the form factors obtainable from any other set of acceptable parameters must be very close to the form factors presented in this paper.

In order to investigate the sensitivity of our results to the effective value of the ρ mass we looked for the minimum of χ^2 as a function of the parameter M_ρ^2 . This is illustrated in Fig. 3. Each point represents a completely independent search over the 5 coefficients s_{e1} , s_{e2} , s_{m1} , s_{m2} , and v_{m1} . The sixth coefficient, v_{e1} ,

follows from those parameters through the constraint given by Eq. (6). The numerical values of M_ρ^2 are given in units of F^{-2} , whereas the minimum values of χ^2 are normalized by dividing the actual values by the number of degrees of freedom. The three curves shown correspond to the three combinations of data sets used in the analyses. As can be seen the best result is obtained for combination b, which is a fit to the 114 proton cross sections measured by Janssens *et al.*⁸ and the 71 inelastic electron-deuteron scattering cross sections presented in this paper. Although worse, the result indicated for combination a is still satisfactory. The systematic differences already mentioned between the two data sets for proton cross sections show up in the increased value for χ^2/N for combination c. However, we

TABLE III. Three-pole isotopic form factor model.

	Combination a': Bumiller <i>et al.</i> (58 points)	Combination b': Janssens <i>et al.</i> (114 points) de Vries <i>et al.</i> (71 points) Chen <i>et al.</i> (6 points)	Combination c': Bumiller <i>et al.</i> (58 points) Janssens <i>et al.</i> (114 points) de Vries <i>et al.</i> (71 points) Chen <i>et al.</i> (6 points)
s_{e1}	2.846	2.628	2.944
s_{e2}	-2.183	-1.853	-2.342
s_{m1}	4.727	4.193	4.263
s_{m2}	-4.146	-3.435	-3.543
v_{e1}	1.228	1.191	1.243
v_{m1}	1.090	1.064	1.080
M_p^2	8.628	8.463	8.710
χ^2 Bumiller	100.1		145.4
χ^2 Janssens		115.6	133.1
χ^2 de Vries	54.5	58.2	55.9
χ^2 Harvard	4.2	3.3	3.5
χ^2			
Total	158.8	177.1	337.8
N =number	129	185	243
of degrees			
of freedom			
χ^2/N	1.23	0.96	1.39

cannot at present discriminate against any one of the two sets, since each one separately gives a good fit to the data. The numerical values of the parameters together with the χ^2 values are given in Table II.

In Figs. 4(a) and 4(b) we show the experimental values, $R = (d\sigma/d\Omega)_p / (d^2\sigma/d\Omega dE)_{a,peak}$ given in Table I of this paper. The solid curves are obtained by using the values of the parameters given in Table II for combination a and combination b together with Eqs. (3) and (4). It will be noticed that the two "theoretical" sets of ratios are not significantly different. This is a reflection of the fact that the quantity R is rather weakly dependent on the numerical values of the proton cross sections, i.e., there are sufficiently many free parameters in the model used that R can be fitted quite well for slightly different choices of the proton cross sections.

Recently proton cross sections for q^2 up to $125 F^{-2}$ have been reported by Chen *et al.*³⁸ In order to see if our model is valid in this range of high momentum transfer we have added these data (here referred to as data set IV) to combinations a, b, and c to obtain combinations a', b', and c'. The results obtained by minimizing χ^2 in the latter cases are given in Table III. It is seen that rather small adjustments of the parameters found for combinations a, b, and c suffice to give good fits when data set IV is added. Only combination a' shows an increase in χ^2/N , which could mean that data set I Bumiller *et al.*⁷ suffers from slight systematic errors.

³⁸ K. W. Chen, A. A. Cone, J. R. Dunning, Jr., S. G. F. Frank, N. F. Ramsey, J. K. Walker, and Richard Wilson, Phys. Rev. Letters 11, 561 (1963).

TABLE IV. The error matrix $\langle \Delta x_i \Delta x_j \rangle$ for the parameters determined from the fit to combination b'.

$\begin{matrix} \Delta x_i \\ \Delta x_j \end{matrix}$	s_{e1}	s_{e2}	s_{m1}	s_{m2}	v_{m1}	M_p^2
s_{e1}	0.04128	-0.06255	-0.00888	0.01050	0.00069	0.01292
s_{e2}	...	0.09524	0.01031	-0.01156	-0.00122	-0.02323
s_{m1}	0.03841	-0.05186	0.00155	0.03512
s_{m2}	0.07125	-0.00233	-0.05001
v_{m1}	0.00013	0.00238
M_p^2	0.04924

Thus at this point we find that our model shows some preference for data set II over data set I. Until further work has been done, however, we do not think it is justified to reject data set I completely. (Notice for instance that only two points of data set I at $q^2=18.02 F^{-2}$ at 75° and $q^2=19.42 F^{-2}$ at 145° , give a contribution of 31.8 to the total χ^2 .)

For combination b' we have also performed a more complete error analysis by inverting the matrix

$$M_{ij} = - \frac{1}{2} \frac{\partial^2 (\chi^2)}{\partial x_i \partial x_j},$$

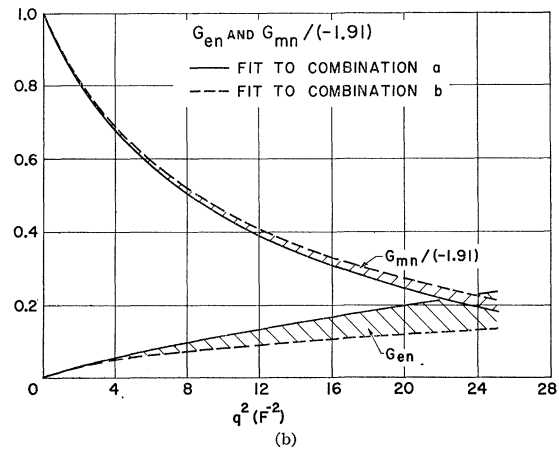
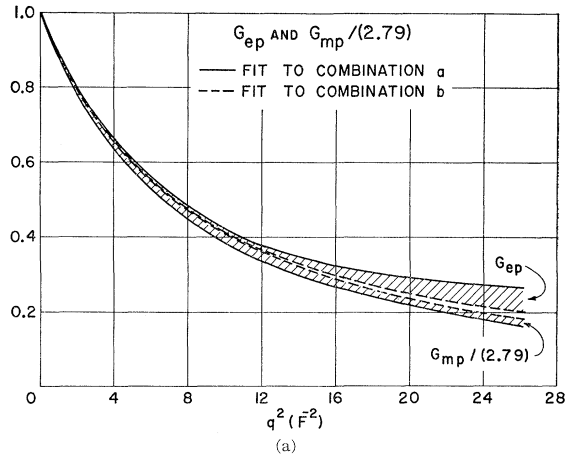


FIG. 5. (a) Charge and magnetic moment form-factor spectra of the proton as obtained from the statistical analyses. (b) Charge and magnetic moment form-factor spectra of the neutron as obtained from the statistical analyses.

where x_i and x_j are two of the six parameters, s_{e1} , s_{e2} , s_{m1} , s_{m2} , v_{m1} , and M_p^2 , v_{e1} being determined by Eq. (6).

The error matrix in Table IV is then given by

$$\langle \Delta x_i \Delta x_j \rangle = c(M^{-1})_{ij},$$

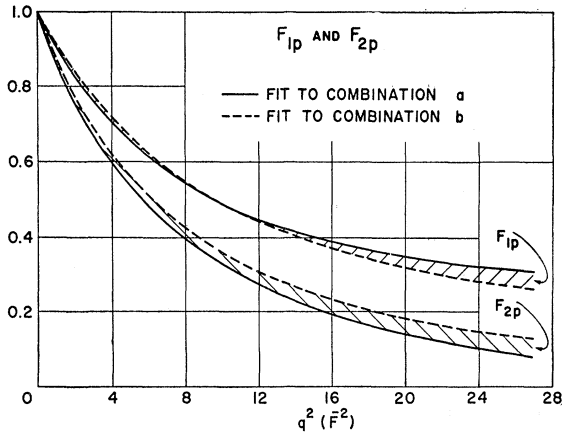
where c is taken to be 1.0 or χ^2/N whichever is larger. Note that $\langle \Delta x_i^2 \rangle^{1/2}$ is just the standard deviation.

V. FORM-FACTOR RESULTS

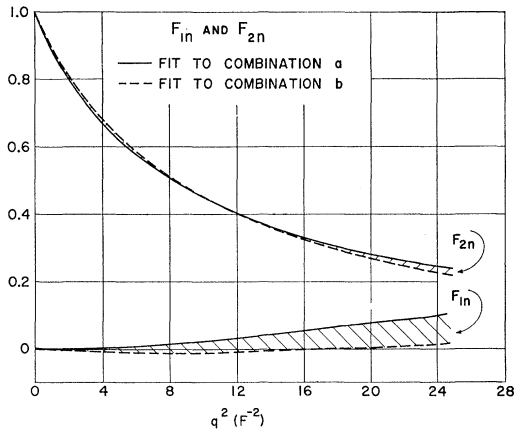
In Figs. 5(a) and 5(b) we have plotted the electric and magnetic form factors of the nucleons obtained from the analysis given in the preceding section. The solid and dashed curves are found by using the parameters given in Table II for the combinations a and b, respectively. Figures 6(a) and 6(b) show the same results in terms of the Dirac and Pauli form factors. Those follow from the electric and magnetic form factors through the relations:

$$G_e = F_1 - (q^2/4M^2)KF_2, \quad (7)$$

$$G_m = F_1 + KF_2, \quad (8)$$



(a)



(b)

FIG. 6. (a) Dirac and Pauli form-factor spectra of the proton. (b) Dirac and Pauli form-factor spectra of the neutron.

TABLE V. The standard deviation for the form factors determined from the fit to combination b'.

q^2 in F^{-2}	ΔG_{ep}	ΔG_{mp}	ΔG_{en}	ΔG_{mn}
5.0	0.004	0.005	0.004	0.009
10.0	0.004	0.003	0.009	0.009
15.0	0.004	0.002	0.014	0.011
20.0	0.005	0.002	0.018	0.014
25.0	0.007	0.003	0.022	0.017
30.0	0.009	0.004	0.025	0.020

where K is the anomalous magnetic moment of the corresponding nucleon. All form factors shown are normalized to unity except the neutron form factors G_{en} and F_{1n} , which are zero at $q^2=0$. The form factors obtained from our best fit to combination b' are very close to those for combination b in the region of q^2 covered by these figures. The bands marked by diagonal lines in the form factor representations are the result of the small discrepancies between the proton cross sections given by Bumiller *et al.*,⁷ and the more recent ones measured by Janssens *et al.*⁸ It is gratifying to note that these discrepancies are not very large and one might conclude that the form factor behavior resulting from all of the Stanford data is rather well established.

Some interesting points may be mentioned:

(a) The numerical values for G_{ep} and $G_{mp}/2.79$ are rather close to each other and as a matter of fact, for the combination b, the ratio of these form factors is close to unity throughout the q^2 region considered.

(b) The neutron form factor F_{1n} seems to be very close to zero. (Combination b' gives slightly negative values for F_{1n} in the region of q^2 considered in Fig. 6.)

(c) The neutron form factor F_{2n} is larger than the Pauli form factor F_{2p} of the proton.

(d) The rms radius of the Dirac distribution of the proton is 0.81 and 0.775 F for the combinations a and b, respectively.

In Table V are given the standard deviations for the form factors obtained by using Table IV and the relation

$$(\Delta G)^2 = \sum_{i,j} \frac{\partial G}{\partial x_i} \frac{\partial G}{\partial x_j} \langle \Delta x_i \Delta x_j \rangle.$$

It is seen from Figs. 5(a) and 5(b) that the differences between the fits of combinations a and b are generally larger than the calculated standard deviation. Thus the uncertainties in the form factors are at the present time mainly due to slight but definite discrepancies between data sets I and II.

It is interesting to extrapolate the nucleon form factors to the limit $q^2 \rightarrow \infty$. If the ideas behind the model used are valid such an extrapolation will tell us the size of possible hard cores or whether we have neglected any contributing resonance. In Table VI we give the asymptotic values of the nucleon form factors found from combinations a', b', and c'.

It is seen that the proton cores are very small and

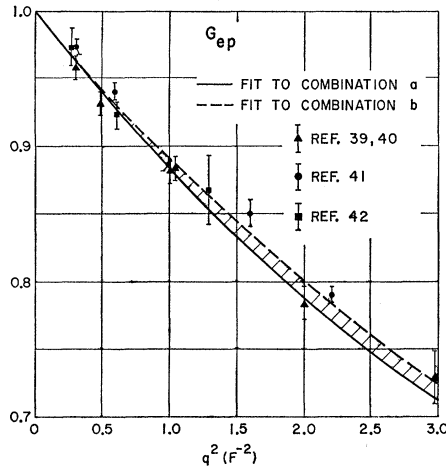


FIG. 7. The present results for G_{ep} on the basis of the statistical analysis described in the text compared with direct measurements of this form factor in the low region of q^2 by Lehmann *et al.* (Ref. 39), Dudelzak *et al.* (Ref. 40), Drickey and Hand (Ref. 41), and Yount and Pine (Ref. 42).

probably not significantly different from zero. The neutron cores are, on the other hand, quite large. One must note in this connection that we only have *proton* data in the region of very high q^2 , which means that only the proton cores are well known. If future neutron data for large q^2 turn out to be consistent with the assumption of no neutron cores, our present model would have to be extended to include another vector resonance in addition to the ρ resonance.

VI. COMPARISON WITH THE RESULTS OF MEASUREMENTS NOT INCLUDED IN THE ANALYSIS

Figure 7 shows the behavior of G_{ep} in the low region of q^2 that follows from the parameters given in Table II for the combinations a and b, and a comparison with experimental results in this region. The data presented are taken from papers of Lehmann *et al.*,³⁹ Dudelzak *et al.*,⁴⁰ Drickey and Hand,⁴¹ and Yount and Pine.⁴² The agreement is very satisfactory. Combination b seems to fit the data slightly better than combination a.

TABLE VI. Asymptotic values of nucleon form factors.

Form factor	Combination a'	Combination b'	Combination c'
G_{ep}	0.054	0.017	0.077
G_{mp}	-0.028	-0.046	-0.065
G_{en}	0.283	0.208	0.321
G_{mn}	0.396	0.257	0.311

³⁹ P. Lehmann, R. Taylor, and R. W. Wilson, Phys. Rev. **126**, 1183 (1962).

⁴⁰ B. Dudelzak, G. Sauvage, and P. Lehmann, Nuovo Cimento **28**, 18 (1963).

⁴¹ C. J. Drickey and L. N. Hand, Phys. Rev. Letters **9**, 521 (1962).

⁴² D. Yount and G. Pine, Phys. Rev. **128**, 1842 (1962).

Combination b' is almost indistinguishable from combination b.

In Fig. 8 we show the experimental proton cross sections obtained by Berkelman *et al.*⁴³ in the region of q^2 from 25–45 F^{-2} . These cross sections have been obtained by measuring the electron in coincidence with the proton. The curved lines are obtained from the results of this paper. The data show a preference for combination b', but there is a pronounced disagreement, especially for the 144° points. This result has stimulated us to perform an analysis of the type described in Sec. IV on the 21 experimental points of Berkelman *et al.*⁴³ alone. We did not succeed in getting a good three-pole isotopic form factor fit. The lowest value of χ^2 obtained was about 35 for 15 degrees of freedom. Using the parameters quoted by Kirson,³⁴ who essentially used the same model for the form factors, the fit was even less satisfactory.

In Fig. 9 we show the results for G_{en} in order to show how our results compare with other information about the behavior of this form factor. It can be seen that the two points measured by Stein *et al.*⁴⁴ do not agree with the results of our analysis. Also the measurements by Drickey and Hand,⁴¹ which indicate that G_{en} is essentially zero in the low region of q^2 , up to 3 F^{-2} , are not in agreement with the behavior shown by our curves. However, this is not surprising, because we have enforced the constraint $(dG_{en}/dq^2)_{q^2=0}=0.021$ on our fits.

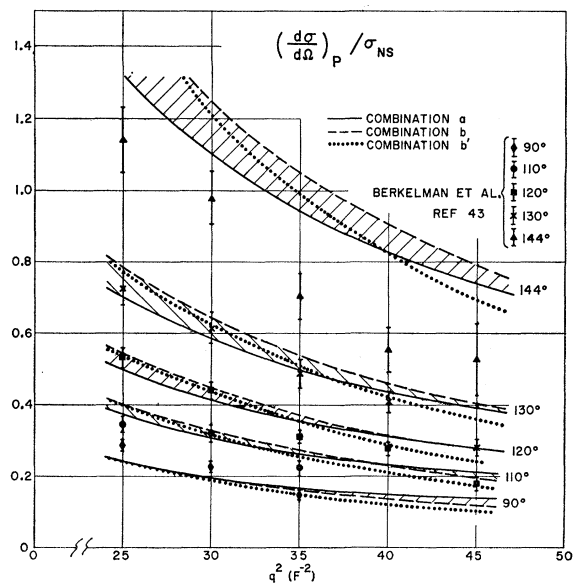


FIG. 8. The quantity $(dI/d\Omega)_p/\sigma_{NS}$ in the region of q^2 from 25–45 F^{-2} . The experimental points are those by Berkelman *et al.* (Ref. 43). The curves are extrapolated fits to electron-proton cross section data in the region of q^2 below 30 F^{-2} .

⁴³ K. L. Berkelman, M. Feldman, R. M. Littauer, G. Rouse, and R. R. Wilson, Phys. Rev. **130**, 2061 (1963).

⁴⁴ P. Stein, R. W. McAllister, B. D. McDaniel, and W. M. Woodward, Phys. Rev. Letters **9**, 403 (1962).

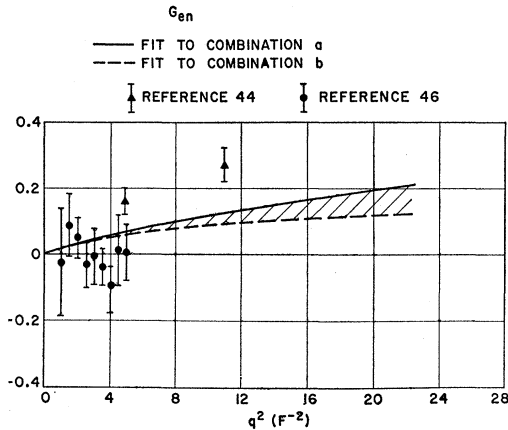


FIG. 9. The present results for G_{en} on the basis of the statistical analysis described in the text compared with direct measurements of this form factor by Stein *et al.* (Ref. 44) and Schiff *et al.* (Ref. 46).

The fact, however, that with this constraint one can obtain very satisfactory fits to the information on neutron form factors given in this paper adds some confidence in the results indicated by our curves. There is some additional information on the neutron form factors given in the results of Griffy *et al.*⁴⁵ Those results for the region of q^2 below 10^{-2} suggest that final state corrections are needed in the Durand expression in order to obtain real neutron form factors. The results of Griffy *et al.* are consistent with those of this paper within experimental error.

Another very interesting result is given by Schiff *et al.*⁴⁶ Values of the electric form factor of the neutron were obtained from an analysis of the experimental electron-tritium and electron-helium-3 cross sections. These points are also shown in Fig. 9.

VII. CONCLUSIONS

The results of the present paper show that the electron-nucleon scattering cross sections in the region of q^2 between 3.0 and 30.0 F^{-2} , measured by Bumiller *et al.*, Janssens *et al.*, and the present authors, can be

⁴⁵ T. A. Griffy, R. Hofstadter, E. B. Hughes, T. Janssens, and M. R. Yearian, in *Proceedings of the Conference on Nucleon Structure* (Stanford University Press, Stanford, California, 1963).

⁴⁶ L. I. Schiff, H. Collard, R. Hofstadter, A. Johansson, and M. R. Yearian, *Phys. Rev. Letters* **11**, 387 (1963).

fitted extremely well by using a three-pole Clementel-Villi model for the isotopic form factors. The same model can in addition, be made to fit the recently measured electron-proton cross sections for q^2 from 45 to 125 F^{-2} with only minor changes in the parameters. Although there still exists a slight systematic discrepancy between the two sets of proton data of Bumiller *et al.* and Janssens *et al.*, the behavior of the proton form factors up to $q^2=30 F^{-2}$ appears to be well established. In the region of q^2 between 30 and 45 F^{-2} we find a significant discrepancy between the experimental results of Berkelman *et al.* and our analysis. We do not understand this discrepancy but we feel that it is an indication of a systematic difference between the experimental work by Berkelman *et al.* and the Stanford work, rather than any inadequacy of the three-pole Clementel-Villi model.

The behavior of the electric form factor of the neutron is less certain than that of the other form factors because (a) the deuteron cross section is only moderately sensitive to the numerical value of this form factor and (b) discrepancies exist between the various experimental methods used to obtain information about this particular form factor. Some attention should be given in the future to clarify the present situation concerning the charge structure of the neutron.

A very interesting conclusion can be drawn from the values of the free parameters found in the statistical analysis. It is not possible to obtain reasonable fits to the experimental material treated in this paper by inserting into the expressions for the isovector form factors, 750 MeV for the mass of the $J=1, T=1$ resonance, the value usually taken for the mass of the ρ meson. The best value we have obtained for the mass of this "pole" is about 600 MeV. This value is in perfect agreement with the value found by Scotti and Wong in their analysis of the nucleon-nucleon interaction. Whether this shift is fundamental or whether it is an indication of another $J=1, T=1$ particle remains an open question.

As reasonable fits for general use we recommend the numerical results of combinations b and b'.

ACKNOWLEDGMENTS

The authors wish to thank the many members of the staff of The High Energy Physics Laboratory at Stanford University for their help in obtaining the data. We also express our appreciation to Mrs. B. Clark for her assistance with many calculations during the early phases of this work.